PROTEINS
STRUCTURE ■ FUNCTION ■ BIOINFORMATICS

Inhibition of interdomain motion in G-actin by the natural product latrunculin: A molecular dynamics study

Sandra Rennebaum and Amedeo Caflisch*

Department of Biochemistry, University of Zürich, Zürich 8057, Switzerland

ABSTRACT

As part of the cytoskeleton, actin is essential for the morphology, motility, and division of eukaryotic cells. Recent X-ray fiber diffraction studies have shown that the conformation of monomeric actin is flattened upon incorporation into the filament by a relative rotation of its two major domains. The antiproliferative activity of latrunculin, a macrolide toxin produced by sponges, seems to be related to its binding to monomeric actin and inhibition of polymerization. Yet, the mechanism of inhibition is not known in detail. Here, multiple explicit water molecular dynamics simulations show that latrunculin binding hinders the conformational transition related to actin polymerization. In particular, the presence of latrunculin at the interface of the two major domains of monomeric actin reduces the correlated displacement of Domain 2 with respect to Domain 1. Moreover, higher rotational flexibility between the two major domains is observed in the absence of ATP as compared to ATP-bound actin, offering a possible explanation as to why actin polymerizes more favorably in the absence of nucleotides.

Proteins 2012; 80:1998–2008.

Key words: actin; conformational transition; domain rotation; motional correlation; latrunculin.

INTRODUCTION

Actin plays an important role in various cellular processes such as cell motility, cell division, muscle contraction, and cytokinesis.[1] It is the most abundant protein in many eukaryotic cells and highly conserved among different organisms. The globular monomeric form, called G-actin, can reversibly assemble to form filamentous actin (F-actin) via a process controlled by a large number of actin-binding proteins. F-actin constitutes an integral part of the cytoskeleton. In tumor cells, the actin filament morphology is substantially altered which, together with its role in cell division, suggests that actin is a potential drug target.[2–5]

The first crystal structure of G-actin was published in 1990,[6] and today there are more than 80 actin crystal structures available in the Protein Data Bank[7] (PDB). Actin polymerization is inhibited by a number of natural products including latrunculins, a class of macrolide toxins produced by sponges in the Red Sea, including the genus *Latrunculia*, whence the name is derived.[8] The crystal structure of the G-actin/latrunculin A complex[9] shows the macrolide binding above the nucleotide binding site between the two major domains of G-actin (Fig. 1, top left), with its unique 2-thiazolidinone moiety buried deep in the cleft (Fig. 2, top). Latrunculins have antiproliferative, antiangiogenic, antimetastatic, and antimicrobial effects.[10–14] In addition, they reduce intraocular pressure in monkeys, such that they may be useful as treatment agents for glaucoma.[15] Aside from naturally occurring latrunculins, several synthetic analogs are likewise capable of disrupting actin filaments.[14,16–18]

Recent X-ray fiber diffraction data show the main conformational change in the G- to F-actin transition to be a relative rotation of the two major domains by about 20°, resulting in a flat actin monomer in the filament.[19] The structural flattening has been confirmed by cryo-EM[20,21] and a recently published F-actin model by Holmes and coworkers.[22]

Several computational studies have investigated the structural features and plasticity of G- and F-actin. Molecular dynamics (MD) simulations have shed light on the influence of the bound nucleotide on actin

Additional Supporting Information may be found in the online version of this article.

Grant sponsor: Swiss National Science Foundation (to A.C.).

*Correspondence to: Amedeo Caflisch, Department of Biochemistry, University of Zürich, Winterthurerstrasse 190, Zürich 8057, Switzerland.
E-mail: caflisch@bioc.uzh.ch

Received 10 February 2012; Revised 22 March 2012; Accepted 30 March 2012
Published online 10 April 2012 in Wiley Online Library (wileyonlinelibrary.com).
DOI: 10.1002/prot.24088

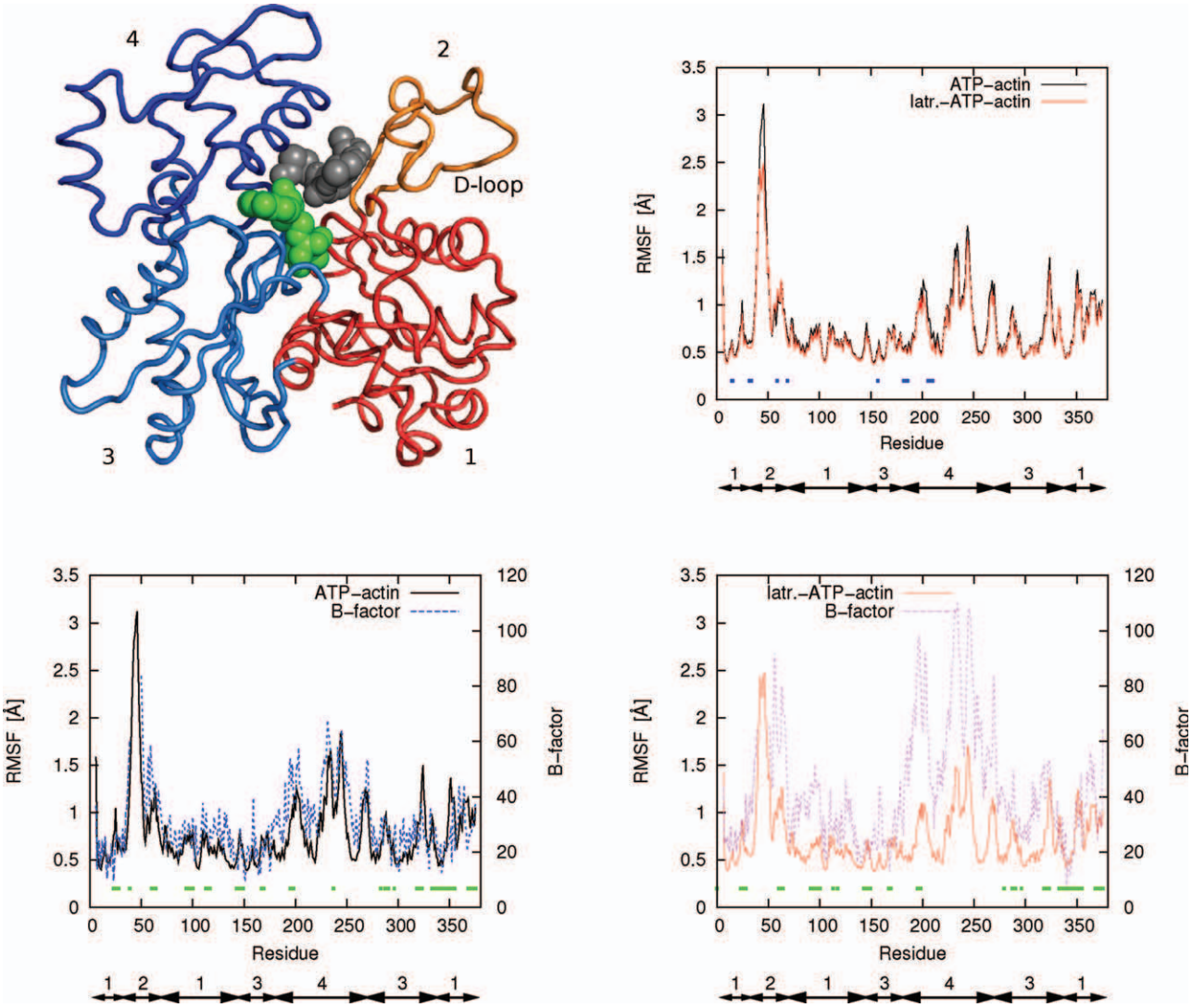

Figure 1

Structure and plasticity of G-actin. (Top, left) Structure of G-actin in complex with latrunculin A based on the 1ESV crystal structure. Actin is conventionally divided into two major domains. Domain 1 consists of Subdomains 1 (residues 1–32, 70–144, and 338–375, shown in red) and 2 (33–69, orange), while Domain 2 consists of Subdomains 3 (145–180 and 270–337, light blue) and 4 (181–269, dark blue). ATP (green) and latrunculin (gray) bind in a cleft between the two domains. (Top, right) RMSFs of C_α atoms in Å as a function of residue number for ATP–actin (black) and latr.–ATP–actin (red). The RMSF values are average values over simulation intervals of 5 ns, and the first 10 ns of each run were neglected. The subdomain numbering is given by the black arrows below the *x*-axis. The blue squares show the residues constituting the latrunculin binding site, that is, those residues with at least 50% of atoms within 5.0 Å of any atom of the inhibitor or residues forming a hydrogen bond to latrunculin in the 1ESV crystal structure (residues Gly15, Leu16, Pro32, Ile34, Gln59, Tyr69, Asp157, Gly182, Arg183, Thr186, Arg206, Glu207, and Arg210). (Bottom left and right) RMSF of C_α atoms in Å (black and red line, respectively, with *y*-axis on the left) and the crystallographic B-factors (blue and magenta dots, respectively, with *y*-axis on the right) for ATP–actin (bottom left) and latr.–ATP–actin (bottom right). Crystal contacts are shown by green squares for residues with one or more heavy atoms closer than 5 Å to heavy atoms of neighboring proteins in the crystal. [Color figure can be viewed in the online issue, which is available at wileyonlinelibrary.com.]

conformation.[23–26] The conformation of the DNase I binding loop (D-loop) is still controversially discussed. Although Zheng *et al.* observed an unfolded D-loop in the ATP-bound and a folded loop in the ADP-bound state,[24] a nucleotide-dependence of the D-loop conformation could not be confirmed by Dalhaimer *et al.*[25] or Splettstoesser *et al.*[26] In a recent metadynamics simulation study, it was found that the folded and unfolded states of the D-loop are similarly stable in ADP–actin.[23] Moreover, MD simulations indicate that the predominant form of G-actin is the closed and twisted conformation, independent of the nature of the bound nucleotide.[25] The open conformation of actin, observed only in complex with profilin, was found to be unstable upon

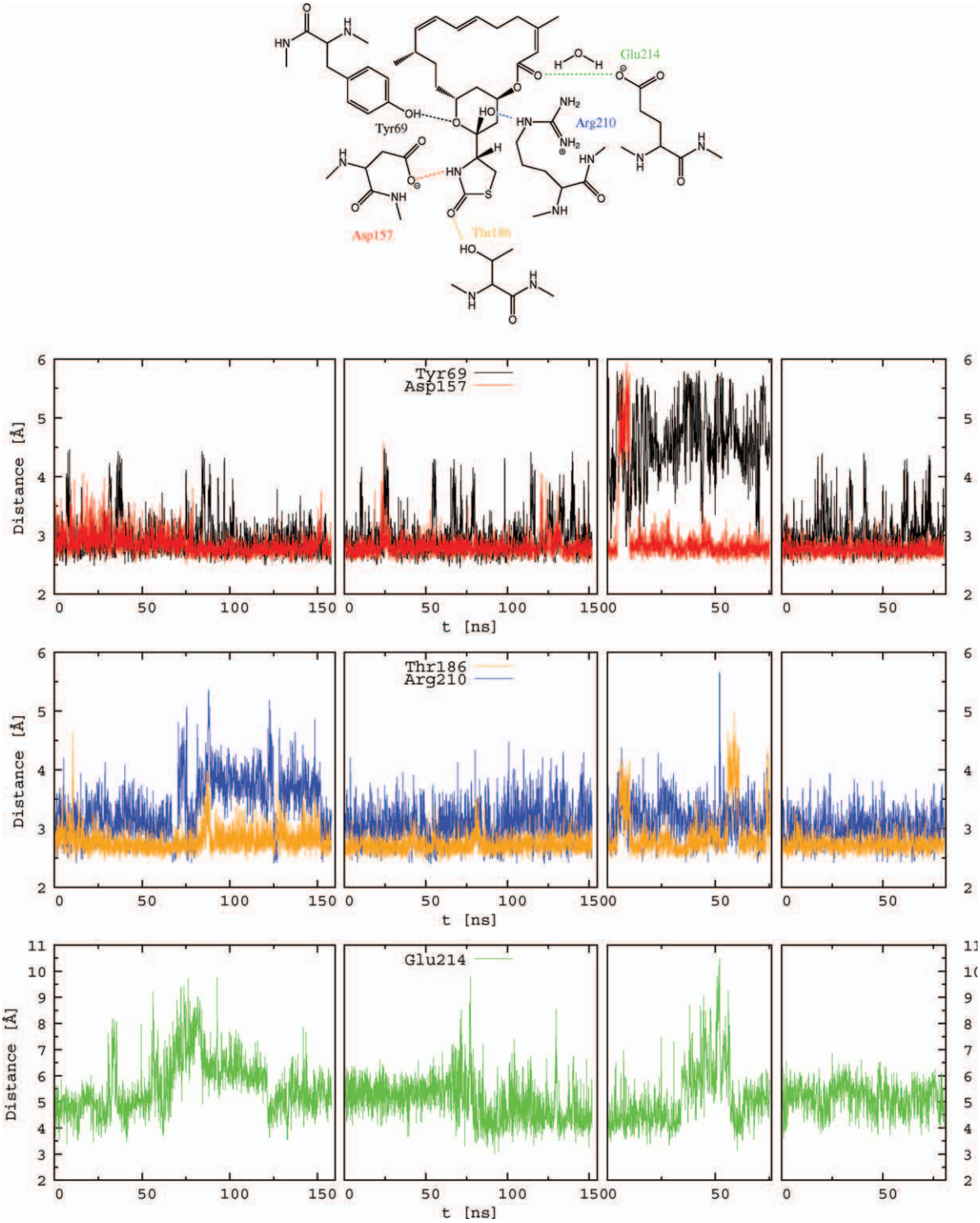

Figure 2

Stability of latrunculin binding mode along MD simulations. (Top) Two-dimensional scheme of latrunculin A and G-actin residues involved in hydrogen bonds. (Middle and bottom) Time series of hydrogen bond distances, that is, the distance between donor and acceptor atoms. The colors are consistent with those used in the top panel. The individual MD runs are shown in separate panels. Note the different *y*-axis range for the hydrogen bond to Glu214, which is water-bridged.

removal of profilin.[26,27] Recent MD studies of the Oda model[19] and the latest Holmes model[22] of F-actin indicate that the interdomain twist of F-actin increases slightly during the simulations.[22,28] However, the twist angle still remains significantly smaller than in G-actin simulations for both models. In recent MD simulations,[26] a "superclosed" G-actin conformation was observed, which resembles the structure in F-actin models.[19–22] Furthermore, water molecules in the nucleotide binding site have been shown to influence actin conformation in MD simulations.[29] The influence of the natural product phalloidin on the actin filament has been investigated by explicit solvent MD simulations.[28] Interestingly, during these simulations a displacement was observed from the original position proposed by the experimentalists toward a site with more adjacent interstrand contacts between subunits along the short-pitch helix, which is congruent with the filament stiffening effect of phalloidin.[28]

As of today, no computational study of the effect of latrunculin on the dynamical properties of G-actin has been reported. Here, we investigate the motional correlation between subdomains in monomeric actin and the influence of latrunculin on the relative rotation of the two major domains by explicit solvent MD simulations. Three systems are investigated in detail: apo actin, ATP-bound actin, and ATP-bound actin in complex with latrunculin A. Multiple MD runs for each system are carried out for a total simulation time of about 1.2 μs. Simulations of nucleotide-free actin indicate a higher interdomain rotational flexibility compared to the ATP-bound state, which is congruent with the observation that nucleotide-free actin polymerizes more favorably than ATP–actin.[30] Moreover, the simulations in the presence of latrunculin show that binding of this natural product prevents the relative rotation of the two major domains, which is necessary for the G- to F-transition, thus interfering with actin polymerization.

MATERIALS AND METHODS

Preparation of the structures

The coordinates of the inhibitor-free[31] and -bound[9] actin were downloaded from the PDB database (PDB ID: 1EQY and 1ESV, respectively). As residues 1–5 are missing in the X-ray structures, the —$COCH_3$ group was added to the N-terminal Thr6. The C-termini were considered negatively charged.

Due to the high flexibility of the D-loop, the coordinates of its residues are not present in the PDB files (residues 40–49 in 1EQY and 40–50 in 1ESV). As in previously published MD studies of G-actin,[23–25,29] initial D-loop coordinates were obtained from an actin crystal structure with the D-loop residues resolved. Using SWISS-MODEL,[32] the PDB structure 3DAW was selected as template for the two following reasons. First, the 1EQY and 1ESV coordinate sets are ATP-bound actin structures, which is also the case for 3DAW. Second, in 3DAW, the protein used for cocrystallization (which is a domain of twinfilin) binds between the actin Subdomains 1 and 3, which are located far away from the D-loop, and thus the presence of the twinfilin domain does not directly influence the conformation of the D-loop. Similar to the procedure described in Ref. 24, after fitting the crystal structures (1EQY and 1ESV) to the template using the C_α atoms present in all structures, the missing coordinates of the D-loop were taken from the template and inserted into the 1EQY and 1ESV structure. To relax elongated bonds after the coordinate transfer, an energy minimization of 100 steps of the steepest descent and 1000 steps of the adopted basis Newton–Raphson algorithm was carried out using the program CHARMM[33,34] and the CHARMM22 force field.[35] During the minimization, all coordinates present in the X-ray structures were kept fixed. Note that in this study, the coordinates of the D-loop are not used for structural alignment or calculation of root mean square deviation (RMSD). As there is no crystal structure of the ATP-free actin available, the coordinates of ATP and the associated calcium ion were removed from the 1EQY structure. The resulting structure is referred to as "apo actin."

MD simulations

To reproduce neutral pH conditions, the side chains of aspartates and glutamates were negatively charged, those of lysines and arginines were positively charged, and histidines were considered neutral. The protein was immersed in an orthorhombic box of pre-equilibrated water molecules. The size of the box was chosen to have a minimal distance of 13 Å between the boundary and any atom of the protein. VMD[36] was used for setting up the simulation system, while minimization, heating, and production runs were performed with NAnoscale Molecular Dynamics (NAMD)[37] using the CHARMM22 force field[35] and the TIP3P model of water. For the parameters of latrunculin A, the CGenFF force field[38] was used. Periodic boundary conditions were applied, and the particle-mesh Ewald approach[39] was used for the long-range electrostatics. The van der Waals interactions were truncated at a cutoff of 12 Å, and a switch function was applied starting at 10 Å. The MD simulations were carried out at constant temperature (310 K) and constant pressure (1 atm) with a time step of 2 fs using the SHAKE algorithm[40] to fix the length of covalent bonds involving hydrogen atoms.

Twist angle

Twist angles between Domains 1 and 2 were calculated as described in Ref. 41, where the twist angle is defined as the angle between two planes, one containing the C_α

atom of residue Gly55 (Subdomain 2) and the axis of rotation, the other containing Glu207 (Subdomain 4) and the axis of rotation. Each MD snapshot was superimposed to the monomeric ADP–actin structure (PDB ID 1J6Z).[41] The axis of rotation was determined between 1J6Z and the F-actin subunit (PDB ID 2ZWH) using DynDom.[42] In addition to the twist angle, time series of the dihedral angle between the centers of mass of the four subdomains (also called "propeller angle"[26]) were computed. The propeller angle time series are very similar to the twist angle time series and therefore not shown.

Motional correlations from MD trajectories

Normalized fluctuation correlations between pairs of C_α atoms were calculated using the DCC[43] algorithm as implemented in WORDOM [see Eq. (10) in Ref. 44]. Their values range from -1 (for a fully anticorrelated motion between two C_α atoms, i.e., motion in opposite direction) through 0 (indicating no correlation) to $+1$ (for a fully correlated motion).

The linear mutual information (LMI)[45,46] algorithm was utilized as a second method to compute motional correlations [see Eq. (11) in Ref. 44]. LMI values vary from 0 indicating lack of any correlation to $+1$, which is complete correlation between atomic displacements. Anticorrelation is not captured by the mutual information measure. Correlations between perpendicular motions are estimated by the LMI but not the DCC method.

It should be noted that the motional correlations depend strongly on the choice of atoms and reference frame for alignment prior to the correlation analysis. The C_α atoms of Domain 1, excluding residues 40–50, were utilized for the alignment to measure the degree of intradomain correlation of Domain 2. The average structure calculated from the MD trajectories was used as reference frame for each system. To test the robustness of the choice of reference frame, the first 20 ns of each trajectory were removed, and the average structure recalculated. Using the resulting structure as reference frame led to essentially identical covariance matrices.

Accession numbers

The structures used in this study were obtained from the PDB database under accession codes 1EQY, 1ESV, 1J6Z, 2ZWH, and 3DAW.

RESULTS AND DISCUSSION

ATP-bound G-actin is considered as reference and most of the analysis focuses on the differences with respect to this system referred to as "ATP-actin." The tripartite complex is called "latr.–ATP–actin" and the nucleotide-free G-actin is called "apo actin." When "F-actin" is mentioned, the Oda model[19] is referred to. Table I gives an overview of the performed MD simulations.

Table I
Summary of Performed MD Simulations

System	Starting str. (PDB ID)	Latrunculin presence	ATP presence	No. of runs[a]	Length (ns)[b]
ATP–actin	1EQY	No	Yes	4	152, 136, 91, 89
Latr.–ATP–actin	1ESV	Yes	Yes	4	158, 152, 75, 80
Apo actin[c]	1EQY	No	No	2	80, 77

[a]Multiple runs were started using different seeds to generate a random distribution of the initial velocities.
[b]The different lengths of the individual runs are due to manual stopping after the first 150 ns or 75 ns.
[c]Since no crystal structure of ATP-free actin is available, the coordinates of ATP and the associated calcium ion were removed from the 1EQY structure.

Overall stability and flexibility

The low values of the C_α RMSD from the X-ray structure of G-actin used as starting conformation indicate that the overall structural stability is preserved in all MD runs (Supporting Information, Fig. S1). Although apo actin denatures in solution,[47] its stability is preserved for the entire duration of the MD simulations. Apo actin was also found to be stable in a previously published MD simulation of 8 ns.[25] As the rate constant of the denaturation is 0.2 s^{-1},[47] unfolding is not expected to occur even in the 100 ns time scale of the present MD simulations. There is a good correlation between the root mean square fluctuation (RMSF) of the C_α atoms along the MD simulations and the crystallographic temperature factors for ATP–actin (Fig. 1). The low RMSD values and reasonable fluctuations indicate that the force field and simulation protocol are adequate for investigating the dynamical properties of G-actin. The nearly perfect overlap of the calculated RMSF of ATP–actin and latr.–ATP–actin (Fig. 1, top right) suggests that latrunculin influences marginally the fluctuations of the actin backbone on the nanosecond time scale. Thus, the higher *B*-factors for the latr.–ATP–actin complex than in the absence of latrunculin, particularly for Subdomain 4, might originate from disorder in the crystal of the former. In all MD runs, the highest mobility is observed for the D-loop (residues 40–50) in Subdomain 2, which is the most flexible part of G-actin, and residues 220–250 in Subdomain 4, in agreement with recently published MD results of the ADP-bound state.[22] The absence of ATP does not have a strong effect on the C_α RMSF either (Supporting Information, Fig. S2).

It is interesting to analyze the stability of the latrunculin binding mode. Latrunculin stays in its binding site for the entire duration of the MD simulations as shown by the RMSD time series of the heavy atoms of latrunculin which oscillate between 1 and 2.5 Å during most of the runs (Supporting Information, Fig. S3). Moreover, the two intermolecular hydrogen bonds between the thiazolidinone ring of latrunculin and the side chains of

Asp157 and Thr186 are stable (Fig. 2). A slightly lower stability is observed for the hydrogen bonds between the tetrahydropyran moiety and the side chains of Tyr69 and Arg210, while the water-bridged hydrogen bond between the lactone carbonyl and the side chain of Glu214 shows relatively strong fluctuations.

Evidence for the hindrance of interdomain rotation by latrunculin

The relative motion between domains can be measured by the RMSD from G-actin and F-actin after overlap of the C_α atoms of Domain 1. In contrast to ATP–actin, only a negligible number of MD snapshots have a RMSD from F-actin below 4 Å in the latrunculin-bound form (Fig. 3, middle). The contrast is even more pronounced between latr.–ATP–actin and apo actin. The percentage of MD snapshots with a RMSD from F-actin below 3.5 Å is 4.7, 4.4, and 0% for apo actin, ATP–actin, and latr.–ATP–actin, respectively. Using a threshold of 4 Å the corresponding values are 15.1, 11.6, and 0.3%. These simulation results suggest that latrunculin binding decreases the probability of the protein adopting an F-actin-like conformation, whereas the absence of ATP increases the probability. The anticorrelation between the RMSD from G- and F-actin suggests that a conformational change increasing the deviation from G-actin augments also the structural similarity to the conformation observed in the filament. According to Figure 3, the degree of anticorrelation for the three investigated systems is the lowest for latr.–ATP–actin and the highest for apo actin. Thus, the presence of latrunculin interferes with the structural rearrangements required for polymerization.

Another interesting measure of the relative motion of the two domains in the MD trajectories is the fluctuation correlation between pairs of residues, which was computed with two different methods (Fig. 4). In contrast to the dynamic cross correlation (DCC) method, the LMI algorithm is able to estimate correlations between perpendicular motions (see "Materials and Methods" section). For ATP–actin a high degree of correlated movement is observed within the major Domain 2, which indicates that Domain 2 moves almost as a rigid body with respect to Domain 1. While the fluctuations of some segments, for example, residues 157–172 and 275–292, appear uncorrelated to the movement of a large part of Domain 2 according to the DCC results, using the LMI method reveals a high degree of correlation and suggests a perpendicular movement of these residues with respect to a large number of residues in Domain 2. The matrix of difference of motional correlation (Fig. 4, bottom) shows a reduced intradomain correlation for Domain 2 in the presence of latrunculin, indicating that Domain 2 moves to a lesser extent as a rigid body relative to Domain 1 in the latrunculin complex.

The relative rotation of the two main domains can also be monitored by the twist angle (Fig. 5), which is defined as the angle between two planes intersecting at the axis of rotation, with one plane containing the C_α atom of residue Gly55 (Subdomain 2) and the other containing the C_α atom of Glu207 (Subdomain 4).[41] The twist angle in F-actin is 8°, and it ranges between 16 and 25° in G-actin (depending on the crystal structure) with an average of 20°. Overall, higher twist angles are observed for latr.–ATP–actin than for ATP–actin. In the simulations of the latter, there are several events where the twist angle is almost reduced to the value in F-actin or even further, resulting in a flattened structure similar to the conformation in the filament. As an example, in the time interval 75–97 ns of the second run of the ATP–actin simulations the twist angle is close to the one of F-actin (Fig. 5(b)). Note also that during this time interval, the RMSD from F-actin and G-actin after superposition of the C_α atoms of Domain 1 (Supporting Information, Fig. S4) are approximately equal. A flat conformation of ATP-bound G-actin has also been observed in 4 out of 20 explicit water MD simulations in a previous study (where it was called a "superclosed" state).[26] The authors suggested that the superclosed state is not the predominant form of ATP–actin in equilibrium, which is a plausible reason why this state has not been observed crystallographically. In contrast to the flattening observed in the absence of latrunculin, over the entire course of the four MD runs of latr.–ATP–actin, the twist angle remained close to or even higher than the one of G-actin. Thus, latrunculin binding to monomeric actin prevents the relative rotation of the two major domains required for the polymerization process. Interestingly, there are simulation segments during which an increase in RMSD from both G- and F-actin relative to the simulation average (Supporting Information, Fig. S1) correlates with an increase in twist angle (e.g., the time intervals 80–90 ns in the first run of ATP–actin, 3–10 ns and 17–24 ns in the fourth run of latr.–ATP–actin, and 33–39 ns in the first run of apo actin). Here, the two major domains of actin rotate in the opposite direction compared to the flattening in the G- to F-actin transition.

Finally, the interdomain rotation occurs most frequently in simulations of apo actin. There are more flattening events in the simulations of the nucleotide-free structure than in those of ATP–actin, though the former sampling is only about one-third of the latter. Moreover, twist angle values of about 5° are reached only in the absence of ATP. These findings suggest that ATP slightly hinders the relative displacements of the two main domains of G-actin.

CONCLUSIONS

Explicit solvent MD simulations of monomeric actin in the presence and absence of latrunculin have been carried out to study the influence of the binding of this natural

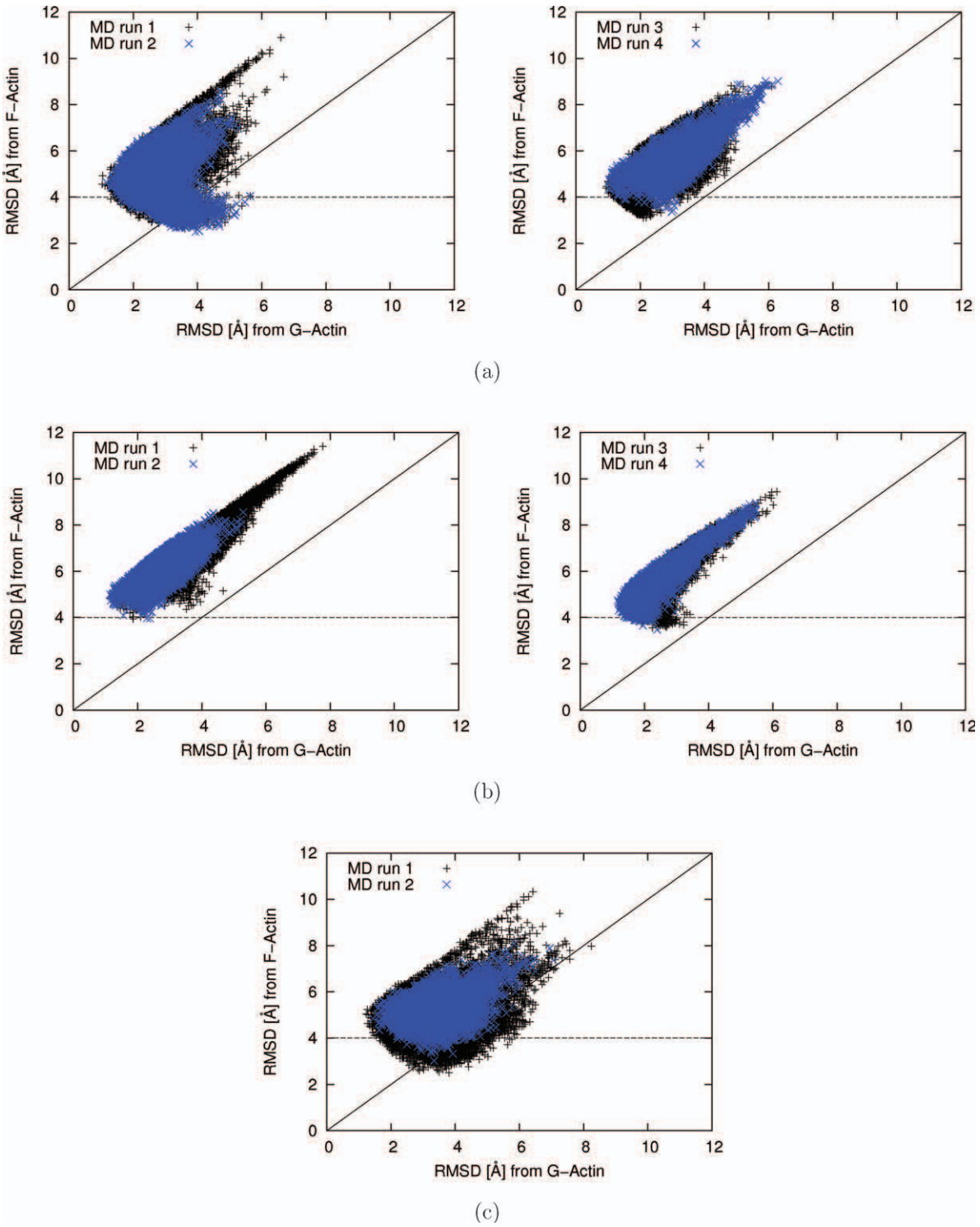

Figure 3

Deviation of MD snapshots from G-actin and F-actin. Scatter plots of RMSD from G- and F-actin, calculated for C_α atoms of Domain 2 upon overlap of C_α atoms of Domain 1 (excluding residues 40–50 of the flexible D-loop), using the structure 2ZWH as reference for F-actin. (**a**) ATP–actin, (**b**) latr.–ATP–actin, and (**c**) apo actin. The reference structure for G-actin is 1EQY in (a) and (c) and 1ESV in (b). For better visibility, MD Runs 3 and 4 are shown separately from Runs 1 and 2 in (a) and (b). [Color figure can be viewed in the online issue, which is available at wileyonlinelibrary.com.]

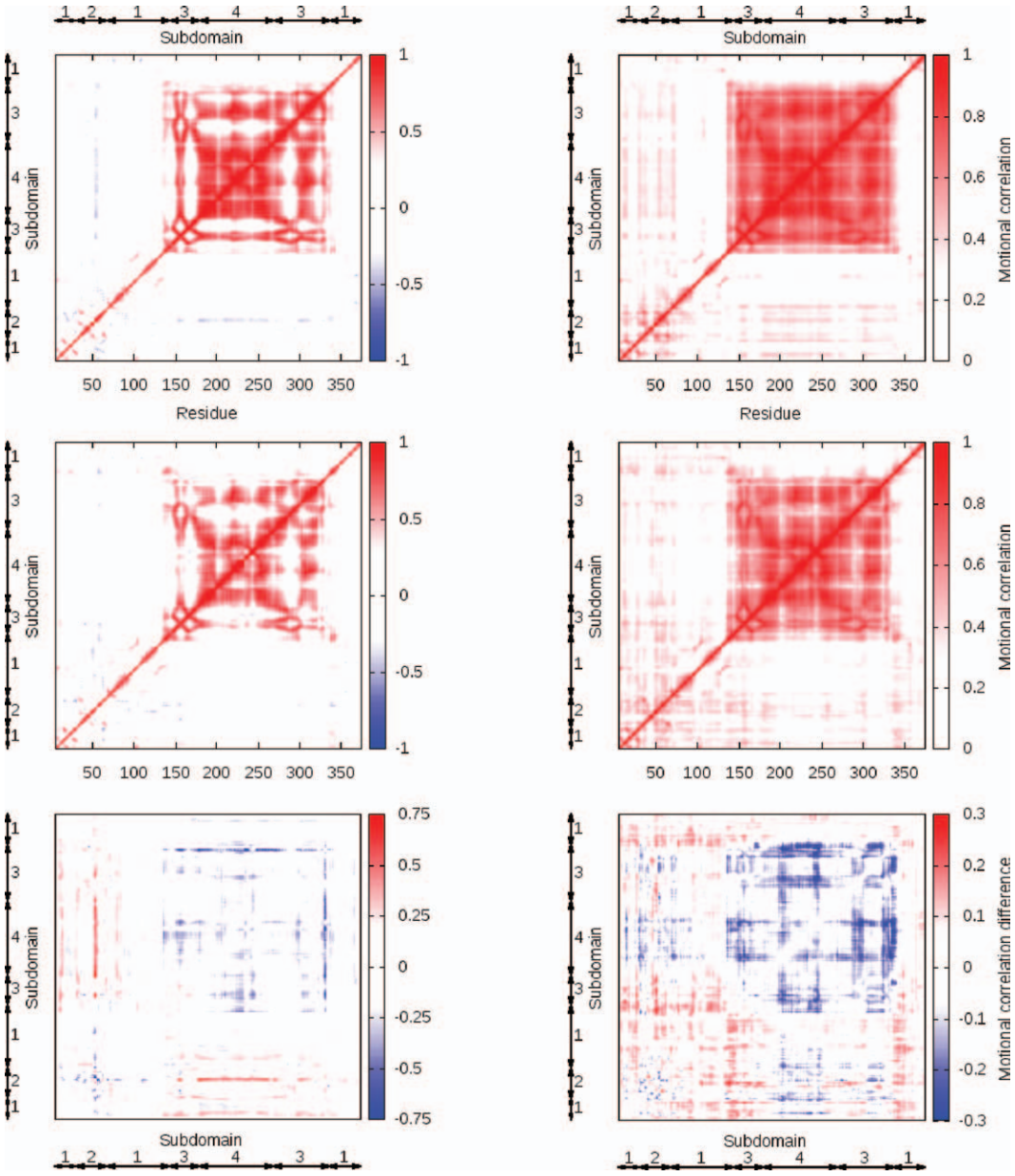

Figure 4

Latrunculin reduces correlated displacement of Domain 2 versus Domain 1. Motional correlations from MD trajectories of ATP–actin (top) and latr.–ATP–actin (middle) calculated by the DCC (left panels) and LMI (right panels) algorithm. The C_α atoms of Domain 1 (excluding the D-loop) were superimposed prior to the correlation analysis. The color scale ranges from blue (anticorrelation) to white (no correlation) to red (correlation) for the DCC algorithm and from white (no correlation) to red (correlation) for the LMI method. The subdomain numbering is given by the black arrows. Note that the two algorithms give similar qualitative results and in particular weaker correlation within the major Domain 2, that is, Subdomains 3 and 4, in the presence of latrunculin. The differences between the two algorithms, and in particular the higher correlation reported by LMI than DCC, originate from the fact that only LMI takes into account correlated perpendicular motion.[44] (Bottom) Difference between motional correlation of latr.–ATP–actin and ATP–actin.

product on the plasticity of G-actin. The simulation results provide evidence that latrunculin prevents actin polymerization by hindering the rotation of the two major domains associated with the G- to F-actin transition. Time series of the twist angle show no substantial flattening for latr.–ATP–actin in contrast to simulations of ATP–actin and apo actin. Moreover, cross correlations of atomic displacements indicate a lower degree of rigid body movement of the two domains relative to each other upon binding of latrunculin. The rotational flexibility of the two domains in G-actin increases in the following order for the three investigated systems: latr–ATP–actin $\ll$ ATP–actin $<$ apo actin.

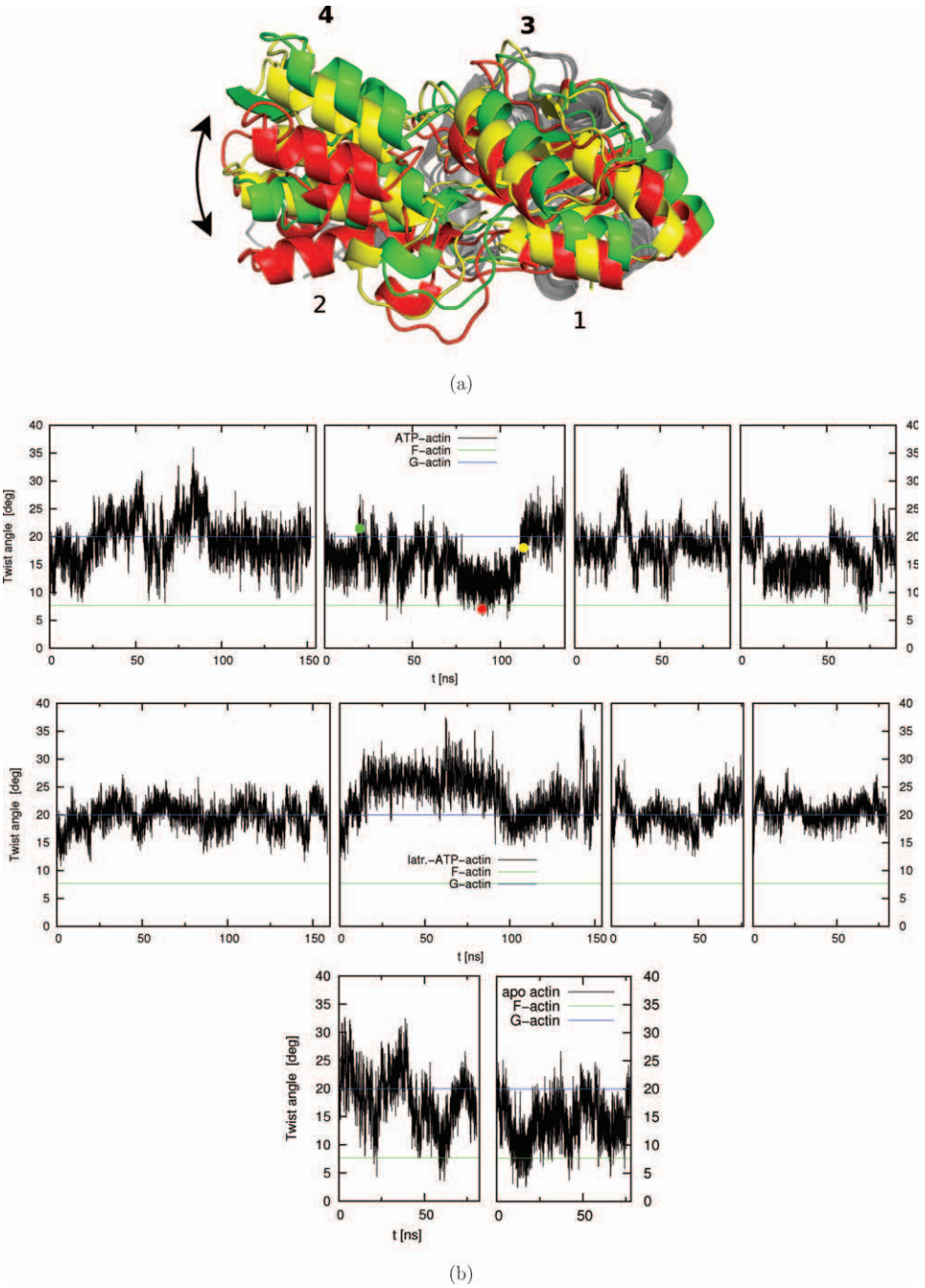

Figure 5

Twist angle analysis shows that latrunculin prevents interdomain motion. (**a**) Side view on Subdomains 3 and 4 of three selected snapshots (green, red, and yellow) from the ATP–actin runs after superposition of C_α atoms of Subdomains 1 and 2 (colored in gray) excluding the D-loop. The arrow illustrates the relative rotation of Subdomain 4. The axis of rotation passes through Subdomains 1 and 3 (not shown). (**b**) Twist angle time series of ATP–actin (top), latr.–ATP–actin (middle), and apo actin (bottom). The three colored circles in the ATP–actin time series correspond to the three snapshots shown in (a). The blue horizontal line shows the mean value of the twist angle measured on 83 crystal structure of G-actin, whereas the green horizontal line indicates the twist angle in the F-actin structure of the Oda model.[19] The individual MD runs are shown in separate panels.

This conclusion is consistent with the experimental observations that nucleotide-free actin polymerizes more easily than ATP-bound actin,[30] whereas latrunculin-bound actin is not able to polymerize.[9]

Considering that both ATP and latrunculin bind in a cleft between the two major domains of monomeric actin, the MD results seem plausible: the domains are able to rotate more freely when their relative movement

is not restricted by the binding of ligands. The inhibitory mechanism of latrunculin proposed here on the basis of the MD simulations could be verified experimentally by mutating one or more of the actin side chains in contact with latrunculin into bulkier ones, for example, Leu16Trp, Ile34Trp, and/or Tyr69Trp. Finally, motivated by the MD simulation results, we are currently carrying out *de novo* design[48] of small molecules that bind in the same cleft as latrunculin as potential anti-cancer compounds.

ACKNOWLEDGMENTS

The authors thank Emilie Frugier and Tim Knehans for carefully reading the manuscript. They thank Dr. Marco Cecchini for interesting discussions and the anonymous reviewers for interesting suggestions. The calculations were carried out on the Schrödinger computer cluster of the University of Zürich (Switzerland).

REFERENCES

1. Schmidt A, Hall MN. Signaling to the actin cytoskeleton. Annu Rev Cell Dev Biol 1998;14:305–338.
2. Jordan MA, Wilson L. Microtubules and actin filaments: dynamic targets for cancer chemotherapy. Curr Opin Cell Biol 1998;10:123–130.
3. Janmey PA, Chaponnier C. Medical aspects of the actin cytoskeleton. Curr Opin Cell Biol 1995;7:111–117.
4. Giganti A, Friederich E. The actin cytoskeleton as a therapeutic target: state of the art and future directions. Prog Cell Cycle Res 2003;5:511–525.
5. Lambrechts A, Van Troys M, Ampe C. The actin cytoskeleton in normal and pathological cell motility. Int J Biochem Cell Biol 2004;36:1890–1909.
6. Kabsch W, Mannherz HG, Suck D, Pai EF, Holmes KC. Atomic structure of the actin: DNase I complex. Nature 1990;347:37–44.
7. Bernstein FC, Koetzle TF, Williams GJB, Meyer EF, Brice MD, Rodgers JR, Kennard O, Shimanouchi T, Tasumi M. The Protein Data Bank: a computer-based archival file for macromolecular structures. J Mol Biol 1977;112:535–542.
8. Nèeman I, Fishelson L, Kashman Y. Isolation of a new toxin from the sponge *Latrunculia magnifica* in the Gulf of Aquaba (Red Sea). Mar Biol 1975;30:293–296.
9. Morton WM, Ayscough KR, McLaughlin PJ. Latrunculin alters the actin-monomer subunit interface to prevent polymerization. Nat Cell Biol 2000;2:376–378.
10. Spector I, Braet F, Shochet NR, Bubb MR. New anti-actin drugs in the study of the organization and function of the actin cytoskeleton. Microsc Res Tech 1999;47:18–37.
11. Longley RE, McConnell OJ, Essich E, Harmody D. Evaluation of marine sponge metabolites for cytotoxicity and signal transduction activity. J Nat Prod 1993;56:915–920.
12. Konishi H, Kikuchi S, Ochiai T, Ikoma H, Kubota T, Ichikawa D, Fujiwara H, Okamoto K, Sakakura C, Sonoyama T, Kokuba Y, Sasaki H, Matsui T, Otsuji E. Latrunculin A has a strong anticancer effect in a peritoneal dissemination model of human gastric cancer in mice. Anticancer Res 2009;29:2091–2097.
13. El Sayed KA, Khanfar MA, Shallal HM, Muralidharan A, Awate B, Youssef DTA, Liu Y, Zhou YD, Nagle DG, Shah G. Latrunculin A and its C-17-O-carbamates inhibit prostate tumor cell invasion and HIF-1 activation in breast tumor cells. J Nat Prod 2008;71:396–402.
14. Khanfar MA, Youssef DTA, El Sayed KA. Semisynthetic latrunculin derivatives as inhibitors of metastatic breast cancer: biological evaluations, preliminary structure–activity relationship and molecular modeling studies. ChemMedChem 2010;5:274–285.
15. Peterson JA, Tian B, Geiger B, Kaufman PL. Effect of latrunculin B on outflow facility in monkeys. Exp Eye Res 2000;70:307–313.
16. Fürstner A, Kirk D, Fenster MD, Aïssa C, De Souza D, Müller O. Diverted total synthesis: preparation of a focused library of latrunculin analogues and evaluation of their actin-binding properties. Proc Natl Acad Sci USA 2005;102:8103–8108.
17. Fürstner A, Kirk D, Fenster MD, Aïssa C, De Souza D, Nevado C, Tuttle T, Thiel W, Müller O. Latrunculin analogues with improved biological profiles by "Diverted otal Synthesis": preparation, evaluation, and computational analysis. Chem Eur J 2007;13:135–149.
18. Amagata T, Johnson TA, Cichewicz RH, Tenney K, Mooberry SL, Media J, Edelstein M, Valeriote FA, Crews P. Interrogating the bioactive pharmacophore of the latrunculin chemotype by investigating the metabolites of two taxonomically unrelated sponges. J Med Chem 2008;51:7234–7242.
19. Oda T, Iwasa M, Aihara T, Maéda Y, Narita A. The nature of the globular- to fibrous-actin transition. Nature 2009;457:441–445.
20. Fujii T, Iwane AH, Yanagida T, Namba K. Direct visualization of secondary structures of F-actin by electron cryomicroscopy. Nature 2010;467:724–728.
21. Murakami K, Yasunaga T, Noguchi TQ, Gomibuchi Y, Ngo KX, Uyeda TQ, Wakabayashi T. Structural basis for actin assembly, activation of ATP hydrolysis, and delayed phosphate release. Cell 2010;143:275–287.
22. Splettstoesser T, Holmes KC, Noé F, Smith JC. Structural modeling and molecular dynamics simulation of the actin filament. Proteins: Struct Funct Bioinform 2011;79:2033–2043.
23. Pfaendtner J, Branduardi D, Parrinello M, Pollard TD, Voth GA. Nucleotide-dependent conformational states of actin. Proc Natl Acad Sci USA 2009;106:12723–12728.
24. Zheng X, Diraviyam K, Sept D. Nucleotide effects on the structure and dynamics of actin. Biophys J 2007;93:1277–1283.
25. Dalhaimer P, Pollard TD, Nolen BJ. Nucleotide-mediated conformational changes of monomeric actin and Arp3 studied by molecular dynamics simulations. J Mol Biol 2008;376:166–183.
26. Splettstoesser T, Noé F, Oda T, Smith JC. Nucleotide-dependence of G-actin conformation from multiple molecular dynamics simulations and observation of a putatively polymerization-competent superclosed state. Proteins: Struct Funct Bioinform 2009;76:353–364.
27. Minehardt TJ, Kollman PA, Cooke R, Pate E. The open nucleotide pocket of the profilin/actin X-ray structure is unstable and closes in the absence of profilin. Biophys J 2006;90:2445–2449.
28. Pfaendtner J, Lyman E, Pollard TD, Voth GA. Structure and dynamics of the actin filament. J Mol Biol 2010;396:252–263.
29. Saunders MG, Voth GA. Water molecules in the nucleotide binding cleft of actin: effects on subunit conformation and implications for ATP hydrolysis. J Mol Biol 2011;413:279–291.
30. De La Cruz EM, Mandinova A, Steinmetz MO, Stoffler D, Aebi U, Pollard TD. Polymerization and structure of nucleotide-free actin filaments. J Mol Biol 2000;295:517–526.
31. McLaughlin PJ, Gooch JT, Mannherz HG, Weeds AG. Structure of gelsolin segment 1-actin complex and the mechanism of filament severing. Nature 1993;364:685–692.
32. Arnold K, Bordoli L, Kopp J, Schwede T. The SWISS-MODEL workspace: a web-based environment for protein structure homology modelling. Bioinformatics 2006;22:195–201.
33. Brooks BR, Bruccoleri RE, Olafson BD, States DJ, Swaminathan S, Karplus M. CHARMM: a program for macromolecular energy, minimization, and dynamics calculations. J Comput Chem 1983;4:187–217.
34. Brooks BR, Brooks CL, MacKerell AD, Nilsson L, Petrella RJ, Roux B, Won Y, Archontis G, Bartels C, Boresch S, Caflisch A, Caves L, Cui Q, Dinner AR, Feig M, Fischer S, Gao J, Hodoscek M, Im W, Kuczera K, Lazaridis T, Ma J, Ovchinnikov V, Paci E, Pastor RW,

Post CB, Pu JZ, Schaefer M, Tidor B, Venable RM, Woodcock HL, Wu X, Yang W, York DM, Karplus M. CHARMM: the biomolecular simulation program. J Comput Chem 2009;30:1545–1614.
35. MacKerell AD, Bashford D, Bellott M, Dunbrack RL, Evanseck JD, Field MJ, Fischer S, Gao J, Guo H, Ha S, Joseph-McCarthy D, Kuchnir L, Kuczera K, Lau FTK, Mattos C, Michnick S, Ngo T, Nguyen DT, Prodhom B, Reiher WE, Roux B, Schlenkrich M, Smith JC, Stote R, Straub J, Watanabe M, Wiórkiewicz-Kuczera J, Yin D, Karplus M. All-atom empirical potential for molecular modeling and dynamics studies of proteins. J Phys Chem B 1998;102:3586–3616.
36. Humphrey W, Dalke A, Schulten K. VMD: visual molecular dynamics. J Mol Graph 1996;14:33–38.
37. Phillips JC, Braun R, Wang W, Gumbart J, Tajkhorshid E, Villa E, Chipot C, Skeel RD, Kalé L, Schulten K. Scalable molecular dynamics with NAMD. J Comput Chem 2005;26:1781–1802.
38. Vanommeslaeghe K, Hatcher E, Acharya C, Kundu S, Zhong S, Shim J, Darian E, Guvench O, Lopes P, Vorobyov I, MacKerell AD. CHARMM general force field: a force field for drug-like molecules compatible with the CHARMM all-atom additive biological force fields. J Comput Chem 2010;31:671–690.
39. Essmann U, Perera L, Berkowitz ML, Darden T, Lee H, Pedersen LG. A smooth particle mesh Ewald method. J Chem Phys 1995;103:8577–8593.
40. Ryckaert JP, Ciccotti G, Berendsen HJC. Numerical integration of the cartesian equation of motion of a system with constraints: molecular dynamics of *n*-alkanes. J Comput Phys 1977;23:327–341.
41. Oda T, Maéda Y. Multiple conformations of F-actin. Structure 2010;18:761–767.
42. Hayward S, Berendsen HJC. Systematic analysis of domain motions in proteins from conformational change: new results on citrate synthase and T4 lysozyme. Proteins: Struct Funct Genet 1998;30:144–154.
43. McCammon JA, Harvey S. Dynamics of proteins and nucleic acids. Cambridge: Cambridge University Press; 1987.
44. Seeber M, Felline A, Raimondi F, Muff S, Friedman R, Rao F, Caflisch A, Fanelli F. Wordom: a user-friendly program for the analysis of molecular structures, trajectories, and free energy surfaces. J Comput Chem 2011;32:1183–1194.
45. Kraskov A, Stögbauer H, Grassberger P. Estimating mutual information. Phys Rev E 2004;69:066138–066154.
46. Lange OF, Grubmüller H. Generalized correlation for biomolecular dynamics. Proteins: Struct Funct Bioinform 2006;62:1053–1061.
47. Kinosian HJ, Selden LA, Gershman LC, Estes JE. Non-muscle actin filament elongation from complexes of profilin with nucleotide-free actin and divalent cation-free ATP–actin. Biochemistry 2004;43:6253–6260.
48. Dey F, Caflisch A. Fragment-based de novo ligand design by multiobjective evolutionary optimization. J Chem Inf Model 2008;48:679–690.